Thermal-mechanical finite element simulation of flat bar rolling coupled with a stochastic model of microstructure evolution

Danuta Szeliga[1]* (iD), Natalia Czyżewska[2] (iD), Jan Kusiak[1] (iD), Roman Kuziak[3] (iD),
Paweł Morkisz[2], Piotr Oprocha[2] (iD), Maciej Pietrzyk[1] (iD), Michał Piwowarczyk[4],
Łukasz Poloczek[3] (iD), Paweł Przybyłowicz[2] (iD), Łukasz Rauch[1] (iD), Natalia Wolańska[4]

[1] AGH University of Science and Technology, Faculty of Metals Engineering and Industrial Computer Science, al. Mickiewicza 30, 30-059 Krakow, Poland.

[2] AGH University of Science and Technology, Faculty of Applied Mathematics, al. Mickiewicza 30, 30-059 Krakow, Poland.

[3] Łukasiewicz Research Network, Institute for Ferrous Metallurgy, ul. K. Miarki 12, 44-100 Gliwice, Poland.

[4] CMC Poland, ul. Piłsudskiego 82, 42-400 Zawiercie, Poland.

Abstract

It is generally recognized that the kinetics of phase transformations during the cooling of steel products depends to a large extent on the state of the austenite after rolling. Austenite deformation (when recrystallization is not complete) and grain size have a strong influence on the nucleation and growth of low-temperature phases. Thus, the general objective of the present work was the formulation of a numerical model which simulates thermal, mechanical and microstructural phenomena during multipass hot rolling of flat bars. The simulation of flat bar rolling accounting for the evolution of a heterogeneous microstructure was the objective of the work. A conventional finite-element program was used to calculate the distribution of strains, stresses, and temperatures in the flat bar during rolling and during interpass times. The FE program was coupled with the stochastic model describing austenite microstructure evolution. In this model, the random character of the recrystallization was accounted for. Simulations supplied information about the distributions of the dislocation density and the grain size at various locations through the thickness of the bars.

Keywords: flat bars, hot rolling, thermal-mechanical finite element model, microstructure evolution, stochastic model

1. Introduction

The main objective of the hot rolling process is to reduce the cross-section of the incoming material to obtain the desired section at the exit from the rolls. Rolling of long products is an important example of rolling processes and includes the rolling of heavy sections, such as channels or I-beams, as well as the rolling of bars and rods with a variety of cross sections. In the latter, which is the topic of our work, billets are rolled into bars or rods of different shapes with a wide spectrum of specialized applications (Lahoti & Pauskar, 2005; Lee, 2004). Bars and rods of various steel grades, usually containing alloying elements, are produced in these mills to fit specialized applications. Beyond the precise shape of the bars and rods, microstructure and

D. Szeliga, N. Czyżewska, J. Kusiak, R. Kuziak, P. Morkisz, P. Oprocha, M. Pietrzyk, M. Piwowarczyk, Ł. Poloczek,
P. Przybyłowicz, Ł. Rauch, N. Wolańska

mechanical properties are crucial parameters in determining the quality of products. The requisite microstructure and mechanical properties are obtained by specific cooling of products, which allows the kinetics of the phase transformations to be controlled. Quite recently, new perspectives have been identified through developing different types of bainitic microstructures or a mixture of ferrite and bainite in long products. To obtain these microstructures, multistage cooling must be applied, including a combination of fast and slow cooling stages (Piwowarczyk et al., 2022). The design of the cooling process is based on the numerical modelling of phase transformations. The kinetics of the transformations depends, to a large extent, on the state of the austenite after rolling. Austenite grain size and deformation (when recrystallization is not complete) have a strong influence on the nucleation and growth of low-temperature phases. Thus, the general objective of the present work was the formulation of a numerical model which simulates the thermal, mechanical, and microstructural phenomena during multi-pass hot rolling of flat bars.

Accounting for the heterogeneity of the microstructure in steels was our particular intention. The relationship between local mechanical properties and microstructural heterogeneities in complex-phase steel has recently been studied intensively (Chang et al., 2021; Hassan & Al-Wadei, 2020). Therefore, in our solution, the thermal-mechanical finite element (FE) program was coupled with the stochastic microstructure evolution model.

Several finite element programs describing the rolling of long products have been published in recent decades (Riljak, 2006; Wisselink et al., 2001) and frequently FE programs were coupled with microstructure evolution models (Chin et al., 1999; Głowacki et al., 1992; Yanagimoto et al., 2000). In all of the published solutions, the local homogeneity of the material was assumed, and average microstructural parameters were determined. On the other hand, it has been shown, for example in the work by Chang et al. (2021), that materials with heterogeneous microstructures have some exceptional properties. As far as steels are concerned, the specific features of heterogeneous microstructures are described in recent papers for multi-phase (Heibel et al., 2018), complex phase (Chang et al., 2021), ferritic/martensitic (Li et al., 2022) and pipeline (Hassan & Al-Wadei, 2020) steels. In all of these publications, deterministic models of microstructure evolution are used. To the best of our knowledge, there have been no publications dealing with the random character of certain microstructural phenomena. Therefore, in our model, we want to account for the heterogeneity of the

material and to predict the distribution of the microstructural parameters instead of their average values. To attain this goal, the random character of the microstructure evolution has to be accounted for. Therefore, coupling of the FE program with the stochastic model of microstructure evolution was an additional objective of the present work. The stochastic model described in publications by Klimczak et al. (2022) and Szeliga et al. (2022a, 2022b) was applied. In these previous works, we concentrated on the development of the mean-field internal variable model, which is based on the stochastic solution of the differential equation and which describes the evolution of dislocation populations. It was shown in the paper by Klimczak et al. (2022) that the introduction of the stochastic variables and accounting for the random character of the recrystallization allows us to predict the heterogeneity of the microstructure of the final product. This feature of the model is important in the design of multi-phase materials. In the publication by Klimczak et al. (2022), the mathematical basis of the model with one stochastic internal variable (dislocation density) was described and the optimal parameters of the numerical solution of the stochastic differential equation were determined. In the work by Szeliga et al. (2022a), grain size was added as the second stochastic internal variable, and an upgraded model for deformation at elevated temperatures was proposed. Identification and validation of that model is also described in the same publication. In another publication by Szeliga et al. (2022b) static recovery and static recrystallization were added, and simulations of multi-step hot forming processes became possible. Moreover, the description of the heterogeneous microstructure of metallic materials using internal independent variables allowed us to account for the history of the process and, as a consequence, predict the features of the microstructure which determine the behaviour of the material at the macro scale. In the present work, the model of Szeliga et al. (2022b) was used to predict distributions of the dislocation density and the grain size at the cross-section of flat bars during hot rolling.

2. Model

The thermal-mechanical-metallurgical model was applied to simulate the hot rolling of flat bars. The thermal-mechanical part of the model uses a finite element (FE) program to calculate distributions of strains, strain rates, stresses and temperatures in the roll gap and temperatures during interpass times. This program was coupled with the stochastic model of Szeliga et al.

(2022b) describing microstructure evolution during the hot forming of steels. Both parts of the model are briefly described below.

2.1. Finite element program

The FE model is based on the rigid-plastic thermo-mechanical approach known as flow formulation proposed in the publication by Kobayashi et al. (1989). The model assumes that the material obeys the Huber–Mises yield criterion and the associated Levy–Mises flow rule. The velocity field in the control volume is determined by searching for a minimum of the power functional (see Kobayashi et al., 1989 for details). The algorithm of the solution and the program used in the present work is described in work by Pietrzyk (2000). The power functional is given by the following equation:

$$J = \int_{\Omega} \left(\sigma_i \dot{\varepsilon}_i + \lambda \dot{\varepsilon}_V \right) d\Omega - \int_{\Gamma} f^T v_s d\Gamma \qquad (1)$$

where: σ_i – effective stress, which is equal to the flow stress σ; $\dot{\varepsilon}_i$ – effective strain rate; Ω – volume; Γ – contact surface; $\dot{\varepsilon}_V$ – volumetric strain rate; λ – Lagrange multiplier; $\mathbf{f}$ – vector of boundary tractions; $\mathbf{v}_s$ – vector of slip velocities at the tool-workpiece contact.

The Levy–Mises flow rule, which is the constitutive law in the FE model, describes the relation between stress ($\boldsymbol{\sigma}$) and strain rate ($\dot{\boldsymbol{\varepsilon}}$) tensors:

$$\sigma = \frac{2}{3} \frac{\sigma}{\dot{\varepsilon}_i} \dot{\varepsilon} \qquad (2)$$

The flow stress σ in Equation (2) is calculated following the KEM model (Estrin & Mecking, 1984; Mecking & Kocks, 1981):

$$\sigma = \alpha M b G \sqrt{\rho_m} \qquad (3)$$

where: b – length of the Burgers vector; G – shear modulus; M – the Taylor factor (≈ 3. for the FCC structure); α – constant called Taylor coefficient hereafter; ρ_m – average dislocation density.

Following the discussion in a publication by Kang & Kim (2019), $\alpha = 0.5$ was assumed in the present work. The accuracy of the model depends, to a large extent, on the correctness of the evaluation of the shear modulus G, which in turn depends on temperature. This modulus influences the relation between σ and ρ_m, see Equation (3). The dependence of the shear modulus G on the temperature has been introduced in (Szeliga et al., 2022a).

2.2. Stochastic model of the microstructure evolution

The stochastic model of the microstructure evolution during hot deformation stems from the Kocks–Estrin–Mecking (KEM) approach (Estrin & Mecking, 1984; Mecking & Kocks, 1981). Dynamic recrystallization was introduced to the model in a publication by Sandström & Lagneborg (1975). In the numerical solution, the recrystallization begins at a certain critical time t_{cr} and the rate of the recrystallization depends on energy accumulated in the material in the time $(t - t_{cr})$ (see Davies, 1994 for details). The whole model is described in our earlier publications, and only the main equations are repeated in the present paper.

In the paper by Czyżewska et al. (2022) we presented a thorough discussion of the solution of the KEM equation for the deterministic variable (average dislocation density). That paper includes the mathematical background and analysis of various approximations of the solution, as well as proof of its convergence and stability. In the work by Szeliga et al. (2021) we included static recovery and static recrystallization in the model and simulations of industrial multi-step hot forming processes could be performed. As discussed in the publication by Klimczak et al. (2022), the deterministic model contains an artificial critical time for dynamic recrystallization t_{cr}, which is not a physical quantity and hence it cannot be measured. It is particularly difficult to interpret when static recrystallization is considered. Therefore, for a more realistic description of the random character of the recrystallization, the stochastic variable $\xi(t_i)$ was introduced (see Klimczak et al., 2022 for details). The stochastic hot deformation model is described in a paper by Szeliga et al. (2022a). After discretization in time, the evolution of the dislocation density is governed by the equation:

$$\begin{aligned} \rho(t_i) &= \rho(t_0)[1 - \xi(t_i)] + \\ &\{\rho(t_{i-1}) + [A_1\dot{\varepsilon} - A_2\rho(t_{i-1})\dot{\varepsilon}^{1-a_7}]\Delta t\}\xi(t_i) \end{aligned} \qquad (4)$$

where: t – time; $\dot{\varepsilon}$ – strain rate.

Coefficients A_1 and A_2 responsible for hardening and recovery are defined in Table 1, where: b – a module of the Burgers vector; Z – Zener Hollomon parameter; l – average free path for dislocations; T – temperature in K; R – universal gas constant; a_1, a_2, a_3, a_9, a_{10} – coefficients. When dynamic recovery is considered, mobility of recovery is proportional to $\dot{\varepsilon}^{-a_7}$ as shown in (Estrin & Mecking, 1984), where $a_7 = 0.25$ is reported. For mathematical reasons, constant coefficient a_2 is introduced in Table 1 and the dependence of the dynamic recovery on the strain rate was moved to Equation (4).

D. Szeliga, N. Czyżewska, J. Kusiak, R. Kuziak, P. Morkisz, P. Oprocha, M. Pietrzyk, M. Piwowarczyk, Ł. Poloczek, P. Przybyłowicz, Ł. Rauch, N. Wolańska

Table 1. Relationships describing coefficients in Equation (4)

Hardening	$A_1 = \dfrac{1}{bl}$ where: $l = a_1 Z^{-a_9}$ $Z = \dot{\varepsilon}\exp\left(\dfrac{a_{10}}{RT}\right)$
Recovery	$A_2 = a_2 \exp\left(\dfrac{-a_3}{RT}\right)$

The parameter $\xi(t_i)$ in Equation (4) accounts for the random character of the recrystallization. The distribution of this parameter is given by:

$$\mathbf{P}\big[\xi(t_i) = 0\big] = \begin{cases} p(t_i) & if \ \ p(t_i) < 1 \\ 1 & otherwise \end{cases}$$
$$\mathbf{P}\big[\xi(t_i) = 1\big] = 1 - \mathbf{P}\big[\xi(t_i) = 0\big] \qquad (5)$$

where: $p(t_i)$ – function which connects the probability that the material point recrystallizes in a current time step with the present state of the material. This function is given by the following equation:

$$p(t_i) = a_4 \times 10^{-10}\, \rho(t_{i-1})^{a_6}\, \frac{3\gamma(t_i)\tau}{D(t_{i-1})}\exp\left(\frac{-a_5}{RT}\right)\Delta t \quad (6)$$

In Equation (6) the coefficient γ represents the fraction of the recrystallized grain boundary which is mobile. It accounts for the grain impingements and depends on the distribution of ξ in the previous time step (see Sandstrom & Lagneborg, 1975):

$$\gamma(t_i) = 1 - \exp\left\{-\mathbf{P}\big[\xi(t_{i-1}) = 0\big] - q\right\}^{a_8}\left\{1 - \mathbf{P}\big[\xi(t_{i-1}) = 0\big]\right\} \ (7)$$

where: a_8 – coefficient, q – a small number representing a nucleus of a recrystallized grain, which is added to avoid zero value of $\gamma(t_i)$ in the case $\mathbf{P}[\xi(t_{i-1}) = 0] = 0$.

It is noteworthy to mention that grain size $D(t_i)$ changes in time, and its evolution is not deterministic but rather follows a (time-dependent) distribution. This makes grain size a second stochastic internal variable, which has an influence on the probability in Equation (7). As already discussed in the work by Klimczak et al. (2022), Equation (6) deals with probability distributions rather than average values of ρ. To calculate those distributions, several solutions of Equation (6) were performed, each time using randomly generated values of $\rho(t_i)$. These individual solutions were then aggregated into histograms at each time step t_i. Numerical tests of this approach for pure copper and for DP steel were performed in the paper by Klimczak et al. (2022), and the optimal numerical parameters such as the number of points, number of bins and number of steps were selected. These findings were adopted in the present work, and 20,000 points were simulated to generate histograms with 10 bins. The number of steps was selected depending on the total time of deformation, assuming the maximum time step of 0.05 s.

In our solution, the initial grain size $D(t_0) \equiv D_0$ which is a random variable. The Weibull distribution was assumed for D_0. The changes in the grain size due to growth were calculated using the equation proposed in work by Sellars (1979):

$$D(t_i) = \left[D(t_{i-1})^{a_{11}} + a_{12}\exp\left(\frac{a_{13}}{RT}\right)\Delta t \right]^{\frac{1}{a_{11}}} \qquad (8)$$

where: $\Delta t = t_i - t_{i-1}$ – time step; $D(t_{i-1})$, $D(t)$ – grain size at the beginning and at the end of the time step, respectively; a_{11}, a_{12}, a_{13} – coefficients.

During the calculation, when the random parameter $\xi(t_i) = 0$, the considered point recrystallizes and its new grain size $D(t_i)$ is drawn from the Gauss distribution with the expected value calculated as dynamically recrystallized grain size:

$$\bar{D}(t_i) = a_{14}Z^{-a_{15}} \qquad (9)$$

where: a_{14}, a_{15} – coefficients.

In the paper by Szeliga et al. (2022b) the model was extended to include interpass times and static phenomena in simulations. Since the strain rate in the interpass time is zero, Equation (4) was modified, and the first term with A_1 responsible for hardening was automatically removed. The second term with A_2 in Equation (4) was modified, accounting for the difference between dynamic and static recovery. Because the strain rate is zero, the term $\dot{\varepsilon}^{(1-a_7)}$ was automatically removed. The mobility of recovery coefficient a_2 was substituted by a_{22}, which was included in the vector of the design variables. The activation energy for self-diffusion a_3 has not changed. In the case of recrystallization, the same coefficients were used for static and dynamic processes (Roucoules et al., 2003). When the random parameter $\xi(t_i) = 0$ during the interpass time, the considered point recrystallizes and its new grain size $D(t_i)$ is drawn from the Gauss distribution with the expected value calculated as statically recrystallized grain size:

$$\bar{D}(t_i) = a_{17}\rho(t_i)^{-a_{18}} D(t_0)^{a_{19}}\exp\left(\frac{a_{20}}{RT}\right)$$

where: a_{14}, a_{15}, a_{18}, a_{19}, a_{20}, a_{21} – coefficients.

The standard deviation σ in the Gauss distribution was the optimization variable a_{16}. The flow of calculations in the model is presented in Figure 1.
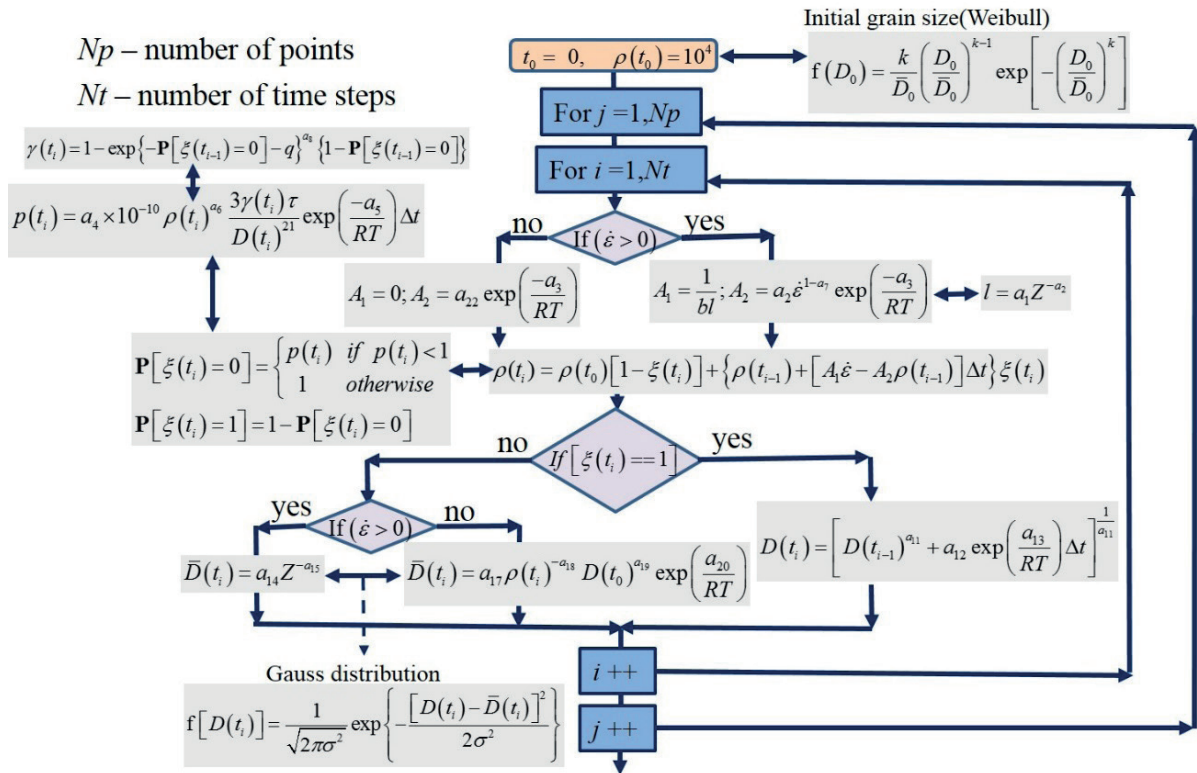
Np – number of points
Nt – number of time steps

$$\gamma(t_i) = 1 - \exp\left\{ -\mathbf{P}\left[\xi(t_{i-1}) = 0\right] - q \right\}^{a_8} \left\{ 1 - \mathbf{P}\left[\xi(t_{i-1}) = 0\right] \right\}$$

$$p(t_i) = a_4 \times 10^{-10} \rho(t_i)^{a_6} \frac{3\gamma(t_i)\tau}{D(t_i)^{21}} \exp\left(\frac{-a_5}{RT}\right) \Delta t$$

$$\mathbf{P}\left[\xi(t_i) = 0\right] = \begin{cases} p(t_i) & if \ p(t_i) < 1 \\ 1 & otherwise \end{cases}$$

$$\mathbf{P}\left[\xi(t_i) = 1\right] = 1 - \mathbf{P}\left[\xi(t_i) = 0\right]$$

Initial grain size(Weibull)

$$f(D_0) = \frac{k}{\bar{D}_0} \left(\frac{D_0}{\bar{D}_0}\right)^{k-1} \exp\left[-\left(\frac{D_0}{\bar{D}_0}\right)^k\right]$$

$t_0 = 0, \quad \rho(t_0) = 10^4$

For $j = 1, Np$

For $i = 1, Nt$

If $(\dot\varepsilon > 0)$ no / yes

$A_1 = 0; A_2 = a_{22} \exp\left(\dfrac{-a_3}{RT}\right)$

$A_1 = \dfrac{1}{bl}; A_2 = a_2 \dot\varepsilon^{1-a_7} \exp\left(\dfrac{-a_3}{RT}\right)$ ↔ $l = a_1 Z^{-a_2}$

$$\rho(t_i) = \rho(t_0)\left[1 - \xi(t_i)\right] + \left\{\rho(t_{i-1}) + \left[A_1\dot\varepsilon - A_2\rho(t_{i-1})\right]\Delta t\right\}\xi(t_i)$$

If $\left[\xi(t_i) == 1\right]$ no / yes

If $(\dot\varepsilon > 0)$ yes / no

$\bar{D}(t_i) = a_{14} Z^{-a_{15}}$

$\bar{D}(t_i) = a_{17}\rho(t_i)^{-a_{18}} D(t_0)^{a_{19}} \exp\left(\dfrac{a_{20}}{RT}\right)$

$$D(t_i) = \left[D(t_{i-1})^{a_{11}} + a_{12}\exp\left(\frac{a_{13}}{RT}\right)\Delta t\right]^{\frac{1}{a_{11}}}$$

Gauss distribution

$$f\left[D(t_i)\right] = \frac{1}{\sqrt{2\pi\sigma^2}} \exp\left\{-\frac{\left[D(t_i) - \bar{D}(t_i)\right]^2}{2\sigma^2}\right\}$$

$i ++$

$j ++$

Fig. 1. Flow chart of the stochastic model

The whole model composed of Equations (4)–(10) contains 22 coefficients $\mathbf{a} = \{a_1, \ldots, a_{22}\}$. Application of the model to real materials requires the identification of the model coefficients. The identification was performed using inverse analysis.

3. Laboratory experiment and industrial rolling process

The laboratory experiments supplied data for the identification and validation of the model. The material was S355J2 steel provided by CMC Poland, and the laboratory experiments composed uniaxial compression tests performed at various temperatures and various strain rates. Details and results of the experiments are described in the work by Poloczek (2022). The identification of the model coefficients was performed using the algorithm developed by the Authors and described in the work by Szeliga et al. (2022a). Coefficients in the

model determined by this algorithm are given in Table 2. The results of the model validation are presented in the publication by Poloczek (2022), and they confirm the good predictive capabilities of the model.

The flat bar production process at CMC Poland was selected as an industrial example. Typical rolling technology for a bar made of S355J2 steel measuring 140 mm × 8 mm was considered. A billet measuring 160 mm × 160 mm was heated in the furnace to obtain a uniform temperature of 1050°C in its volume. A decrease of the preheating temperatures from 1150°C to 1050°C allowed the reduction of the austenite grain growth during interpass times due to the low band temperature. The rolling was performed in 17 passes alternatively in vertical and horizontal stands. The whole process was simulated, and the results for the last five horizontal passes (9, 11, 13, 15 and 17) are presented below. The reductions in these passes were 0.27; 0.18; 0.22; 0.17 and 0.16. The time intervals between passes were 12 s; 6 s; 27 s and 4 s.
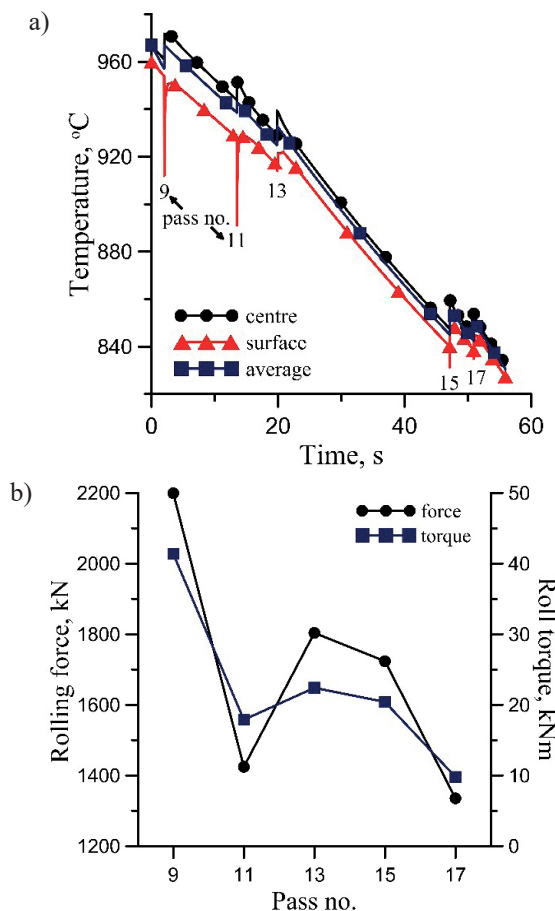
Table 2. Optimal coefficients in the stochastic model

a_1	a_2	a_3	a_4	a_5	a_6	a_7	a_8
1.14	207,864	202,149	4.27×10^{-10}	287,680	1.803	0.273	0.888
a_9	a_{10}	a_{11}	a_{12}	a_{13}	a_{14}	a_{15}	a_{16}
0.288	316,802	2.614	0.3925×10^{11}	458,422	41,096	0.26	18.8

D. Szeliga, N. Czyżewska, J. Kusiak, R. Kuziak, P. Morkisz, P. Oprocha, M. Pietrzyk, M. Piwowarczyk, Ł. Poloczek,
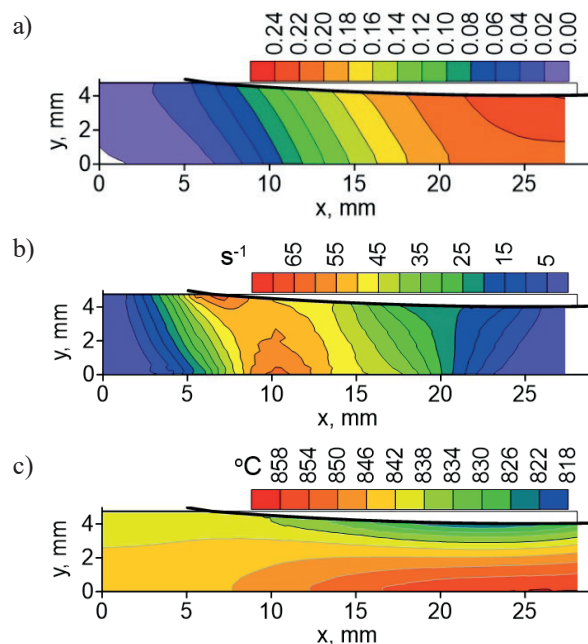P. Przybyłowicz, Ł. Rauch, N. Wolańska

4. Results

4.1. Thermomechanical parameters

Finite element simulations were performed for all horizontal passes. It was observed that finishing passes mostly influence the final microstructure of the bar, and specifically, impact toughness, therefore, the results for the last five passes only are presented below. Calculated temperatures for these passes are shown in Figure 2a, and calculated mechanical parameters are shown in Figure 2b. The temperatures were calculated in the half width of the bar. The finite element program calculates the distributions of strains, strain rates, stresses, and temperatures in the roll gap. These distributions are transferred to the module calculating the austenite microstructure evolution of the rolling process. An example of the calculations of strains, strain rates, and temperatures in the last pass is shown in Figure 3. Due to symmetry, only the top half of the roll gap is presented. The stochastic microstructure evolution model was implemented in the FE program, and calculations of the distributions of dislocation density and grain size were performed. For details, see the results in the next section.

Fig. 3. Distributions of strains (a), strain rates (b) and temperatures (c) in the roll gap in the last pass calculated by the FE program in the plane of symmetry of the bar

4.2. Microstructure evolution

Temperature and strain rate history calculated by the FE model was used as input for the stochastic model of microstructure evolution. As a consequence, the distributions of the dislocation density and the grain size at various locations through the bar thickness could be determined. Only the results for the centre of the bar and for the horizontal passes are presented below.

Calculated distributions of the dislocation density and the grain size at various stages of the finishing rolling are presented in Figures 4–9. All these results are for the centre of the bar. Histograms after pass 9 are shown in Figure 4. Temperature in this pass increased temporary from 960°C to 972°C and the true strain was 0.36. The histograms show that dynamic recrystallization was initiated in this pass, and the metadynamic recrystallization was almost completed in the first second after exit. Histograms after the pass no. 11 are shown in Figure 5. The temperature in this pass increased from 944°C to 951°C, and the true strain was 0.24. Histograms show that the dynamic recrystallization is negligible, and the static recrystallization again was almost completed in the first second after exit. Histograms after the pass no. 13 are shown in Figure 6. The temperature in this pass in the centre of the bar increased from 929°C to 939°C, and the true strain was 0.28. Histograms show that

Fig. 2. Calculated temperatures (a) and mechanical parameters (b) the last five horizontal passes

dynamic recrystallization was not launched, and the static recrystallization was completed in the first second after exit. Due to the long interpass time (over 25 s) grain growth was observed before entry to pass no. 15. Histograms after pass no. 15 are shown in Figure 7. The temperature in the centre of the bar in this pass increased from 848°C to 860°C, and the true strain was 0.23. The histograms show that dynamic recrystallization was not launched, and the static recrystallization was almost completed before entry to pass no. 17. Histograms during pass no. 17 after

strains of 0.05, 0.1 and 0.15 are shown in Figure 8. These results show that dynamic recrystallization is not launched, and the grain size does not change. Histograms after pass no. 17 (the final pass) are shown in Figure 9. The temperature in the centre of the bar in this pass increased from 844°C to 854°C, and the true strain was 0.19. Histograms confirmed observations in Figure 8. The static recrystallization was completed in a time slightly above 1 s, and the microstructure at the beginning of the phase transformations was fully recrystallized.
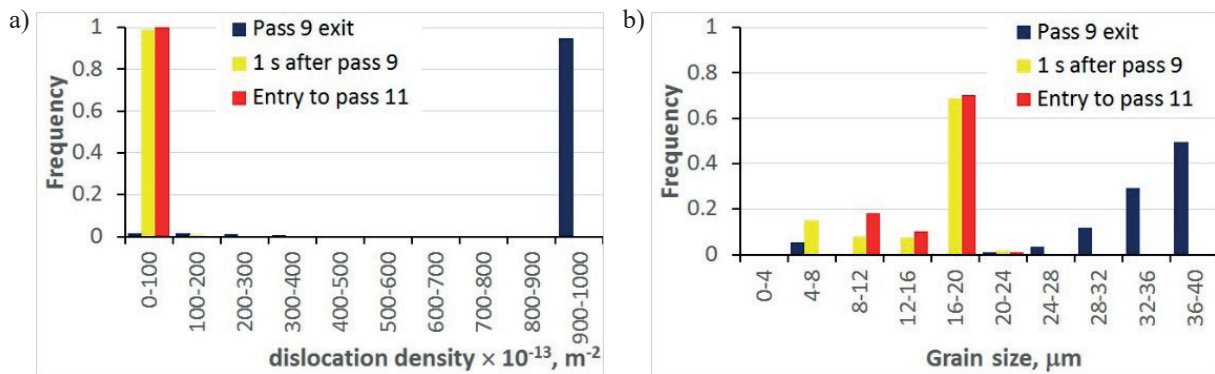

Fig. 4. Distributions of the dislocation density (a) and the grain size (b) at the exit from pass no. 9, 1 s after the exit from this pass and at the entry to pass no. 11
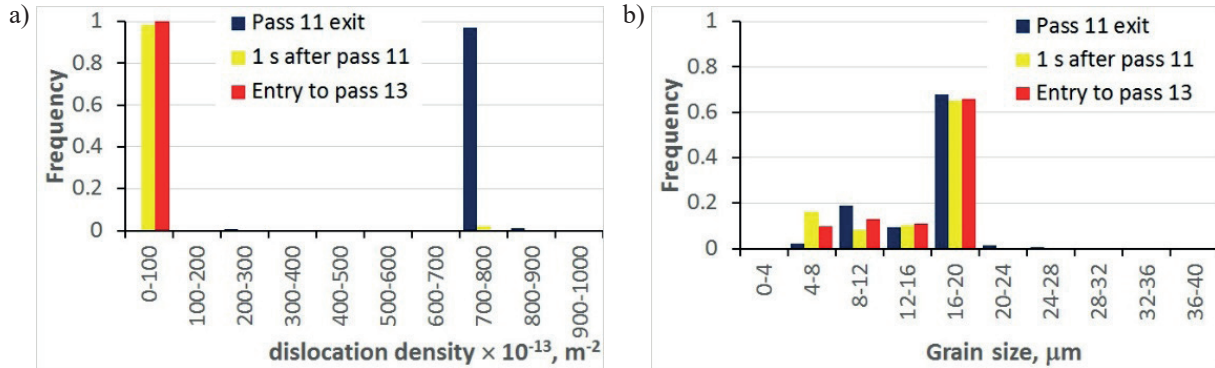

Fig. 5. Distributions of the dislocation density (a) and the grain size (b) at the exit from pass no. 11, 1 s after the exit from this pass and at the entry to pass no. 13
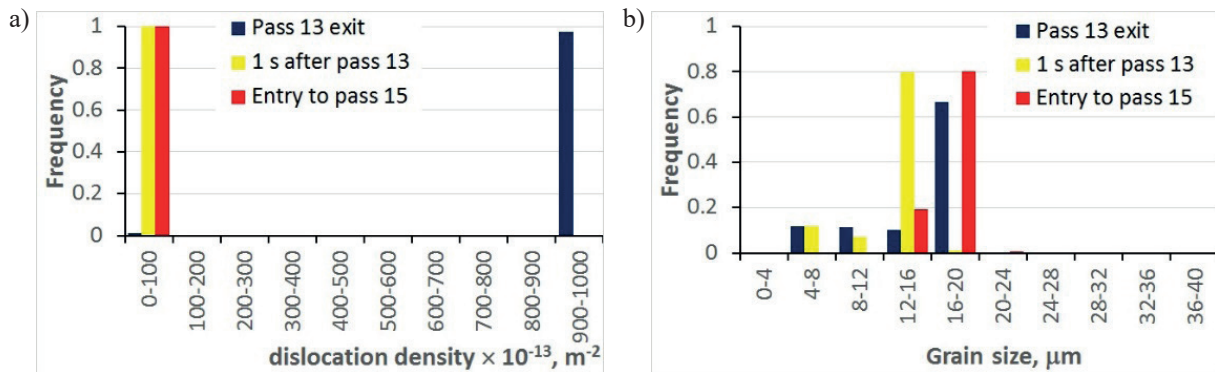

Fig. 6. Distributions of the dislocation density (a) and the grain size (b) at the exit from pass no. 13, 1 s after the exit from this pass and at the entry to pass no. 15
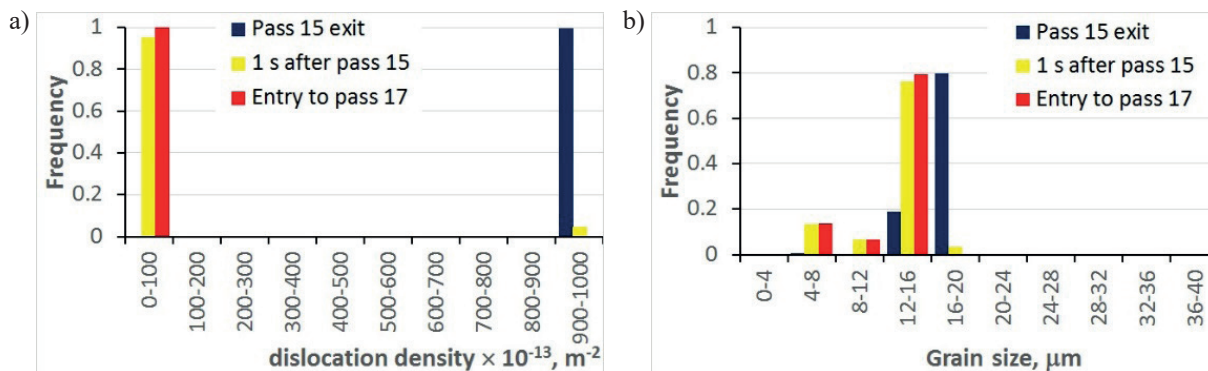
D. Szeliga, N. Czyżewska, J. Kusiak, R. Kuziak, P. Morkisz, P. Oprocha, M. Pietrzyk, M. Piwowarczyk, Ł. Poloczek,
P. Przybyłowicz, Ł. Rauch, N. Wolańska

Fig. 7. Distributions of the dislocation density (a) and the grain size (b) at the exit from pass no. 15,
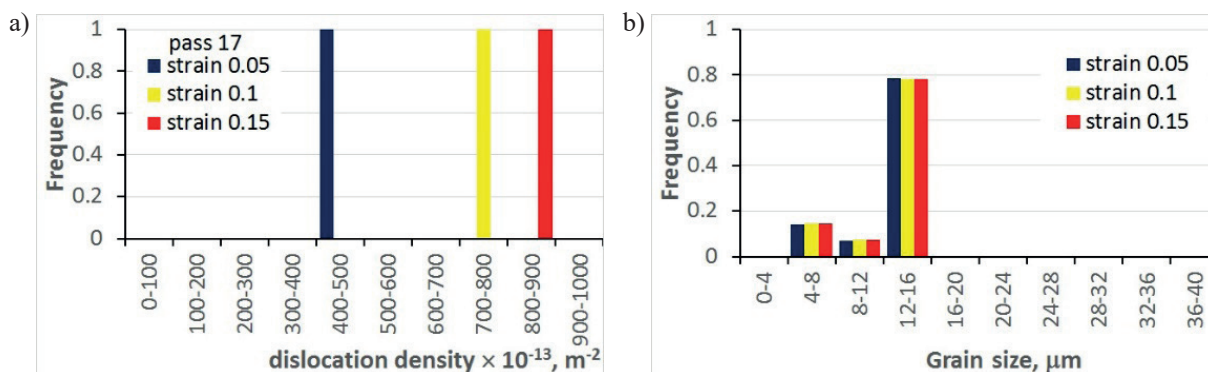1 s after the exit from this pass and at the entry to pass no. 17

Fig. 8. Distributions of the dislocation density (a) and the grain size (b) during pass no. 17, after the strain of 0.05, 0.1 and 0.15
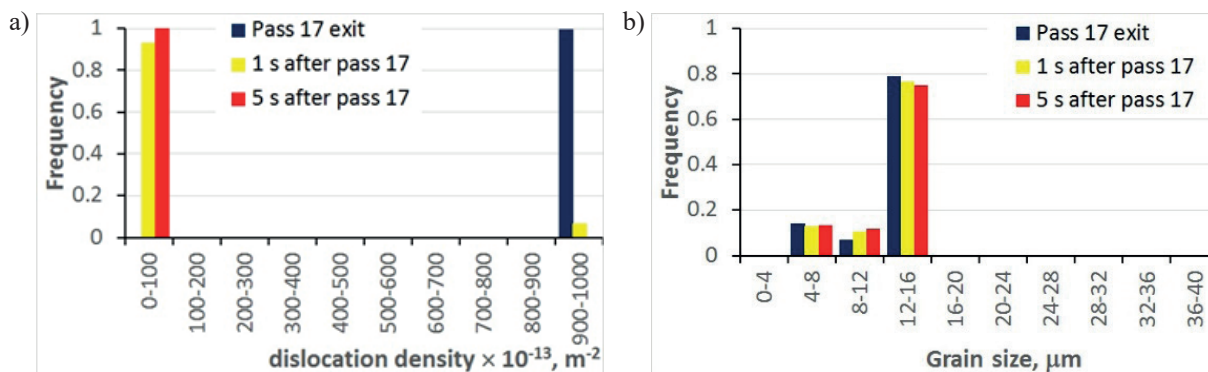

Fig. 9. Distributions of the dislocation density (a) and the grain size (b) at the exit from pass no. 17,
1 s after the exit from this pass and 5 s after the exit from this pass

Fig. 10. Distributions of the dislocation density (a) and the grain size (b) at the exit from pass no. 17,
1 s after the exit from this pass and 5 s after the exit from this pass – preheating temperature decreased by 50°C.
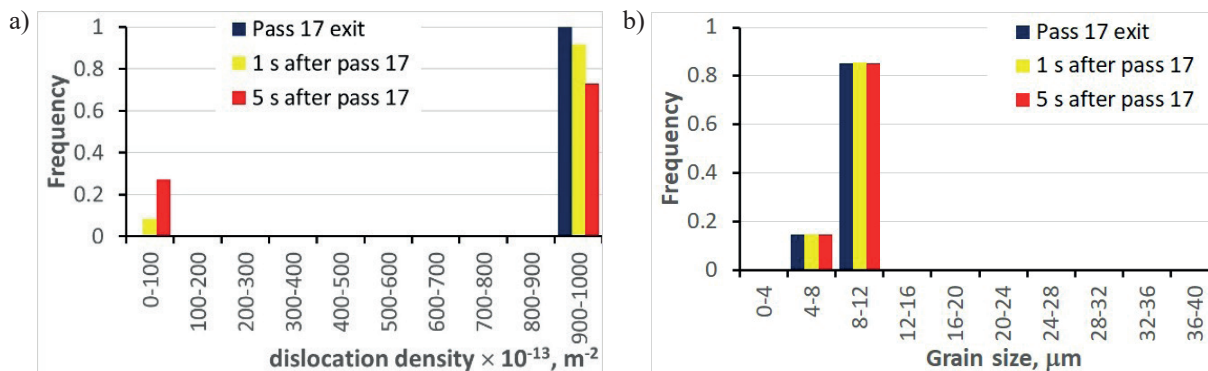
Further simulations were performed to show the model's sensitivity to the process parameters. The preheating temperature was further decreased by 50°C which resulted in a decrease of the temperature in the finishing passes by about 35°C. Results for only the last (17th) pass are presented in Figure 10. It can be seen that recrystallization was retarded compared to the results shown in Figure 9. In 5 s after the exit from the roll gap only 25% of the material has recrystallized. The grain size was finer compared to Figure 9, and it changed only slightly over time.

5. Discussion of results

In the present paper, the mean-field stochastic model described in the works by Szeliga et al. (2022a, 2022b) was implemented into the finite element program, and simulations of multi pass rolling of flat bars were performed. Although the stochastic approach can still be classified as a mean field microstructure evolution model, it supplies additional information about distributions of the internal variables which cannot be obtained from conventional models. For the average values of the microstructural parameters, the model reproduced results similar to those obtained from deterministic mean field models. However, the stochastic model gave a more detailed description of the material in the form of histograms of the microstructural parameters. Validation of the model was performed in the work by Poloczek et al. (2022), and the very good predictive capability of the model was confirmed. Direct verification of the model in the industrial conditions was not possible, but the analysis of the results has shown that they agree qualitatively with our knowledge regarding hot flat bar rolling. The dynamic recrystallization was initiated in passes 1–9, and the metadynamic recrystallization was almost complete during the first second after exit. The dynamic recrystallization was not launched in passes 15 and 17 (smaller strains, lower temperatures), but static recrystallization was almost complete before entry to pass no. 17. The histograms show that static recrystallization was complete in a time slightly above 1 s. Thus, it can be seen that, in the conventional processes, the recrystallization was completed in the centre of the flat bar during the whole process. As a result, the material was recrystallized at the beginning of transformations during cooling, and only grain size distribution should be accounted for in the phase transformation model, which will be the next stage of the development of the model. Simulations for the lower temperatures confirmed the model's sensitivity to the rolling parameters. The significant retardation of the recrystallization was obtained when the preheating temperature was decreased by 50°C.

6. Conclusions

The following conclusions have been drawn on the basis of this research:
- The simulations performed confirmed the capabilities of the model to predict the distribution of microstructural parameters at various stages of hot rolling of flat bars.
- Simulations of the hot rolling of flat bars showed that dynamic recrystallization occurs in the centre of the band in the first passes of the finished rolling (these results are not shown in the paper). The effect of the dynamic recrystallization decreases in subsequent passes, which is due to a decrease of the temperature and an increase in the strain rate.
- Static recrystallization was completed during interpass times and about 1 s after the last pass.
- The stochastic model can be used to design the rolling of flat bars process, which gives the required distribution of selected microstructural parameters in the final product.

The kinetics of phase transformations depends strongly on the condition of the austenite. Therefore, histograms of the dislocation density and the grain size calculated by the stochastic model can be used as input data for the simulation of phase transformations during cooling. This problem will be the subject of our future work.

The mathematical basis of the model is general. The numerical solution of the stochastic evolution equation with can be applied to any variables which are random. Furthermore, the model can be extended to include the effect of austenite grain size distribution following the billet preheating prior to rolling, as well as elements segregation in the initial microstructure. The segregation bands are the result of the non-equilibrium solidification of the billet in the continuous casting process. These bands are characterized by a higher content of C, Mn, and other alloying elements than the average steel composition. This affects the austenite microstructure evolution and phase transformations. Further extensions of the model will include the microstructural parameters concerning pearlite (grain and colony size, interlamellar spacing of cementite), bainite, and martensite (lath width and packet size).

Acknowledgements

D. Szeliga, N. Czyżewska, J. Kusiak, R. Kuziak, P. Morkisz, P. Oprocha, M. Pietrzyk, M. Piwowarczyk, Ł. Poloczek,
P. Przybyłowicz, Ł. Rauch, N. Wolańska

References

Chang, Y., Lin, M., Hangen, U., Richter, S., Haase, C. & Bleck, W. (2021). Revealing the relation between microstructural heterogeneities and local mechanical properties of complex-phase steel by correlative electron microscopy and nanoindentation characterization. *Materials & Design*, *203*, 109620. https://doi.org/10.1016/j.matdes.2021.109620.

Chin, B., Nemes, J.A. & Yue, S. (1999). Influence of strain distribution on microstructure evolution during rod-rolling. *International Journal of Mechanical Sciences*, *41*(9), 1111–1131. https://doi.org/10.1016/S0020-7403(98)00085-X.

Czyżewska, N., Kusiak, J., Morkisz, P., Oprocha, P., Pietrzyk, M., Przybyłowicz, P., Rauch, Ł. & Szeliga, D. (2022). On mathematical aspects of evolution of dislocation density in metallic materials. *IEEE Access*, *10*, 86793–86812. https://doi.org/10.1109/ACCESS.2022.3199006.

Davies, C.H.J. (1994). Dynamics of the evolution of dislocation populations. *Scripta Metallurgica et Materialia*, *30*(3), 349–353. https://doi.org/10.1016/0956-716X(94)90387-5.

Estrin, Y. & Mecking, H. (1984). A unified phenomenological description of work hardening and creep based on one-parameter models. *Acta Metallurgica*, *32*(1), 57–70. https://doi.org/10.1016/0001-6160(84)90202-5.

Głowacki, M., Kedzierski, Z., Kusiak, H., Madej, W. & Pietrzyk, M. (1992). Simulation of metal flow, heat transfer and structure evolution during hot rolling in square-oval-square series. *Journal of Materials Processing Technology*, *34*(1–4), 509–516. https://doi.org/10.1016/0924-0136(92)90148-L.

Hassan, S.F. & Al-Wadei, H. (2020). Heterogeneous microstructure of low-carbon microalloyed steel and mechanical properties. *Journal of Materials Engineering and Performance*, *29*(11), 7045–7051. https://doi.org/10.1007/s11665-020-05217-7.

Heibel, S., Dettinger, T., Nester, W., Clausmeyer, T. & Tekkaya, A.E. (2018). Damage mechanisms and mechanical properties of high-strength multi-phase steels. *Materials*, *11*(5), 761. https://doi.org/10.3390/ma11050761.

Kang, J.-H. & Kim, S.-J. (2019). Critical Assessment 33: Dislocation density-based constitutive modelling for steels with austenite. *Materials Science and Technology*, *35*(10), 1128–1132. https://doi.org/10.1080/02670836.2019.1618030.

Klimczak, K., Oprocha, P., Kusiak, J., Szeliga, D., Morkisz, P., Przybyłowicz, P., Czyżewska, N. & Pietrzyk M. (2022). Inverse problem in stochastic approach to modelling of microstructural parameters in metallic materials during processing. *Mathematical Problems in Engineering*, 9690742. https://doi.org/10.1155/2022/9690742.

Kobayashi, S., Oh, S.-I. & Altan, T. (1989). *Metal Forming and the Finite Element Method*. Oxford University Press.

Lahoti, G.D. & Pauskar, P.M. (2005). Flat, bar, and shape rolling. In S.L. Semiatin (Ed.), *Metalworking: Bulk Forming* (pp. 459–479). ASM International, Materials Park.

Lee, Y. (2004). *Rod and Bar Rolling: Theory and Application*. Marcel Dekker.

Li, S., Vajragupta, N., Biswas, A., Tang, W., Wang, H., Kostka, A., Yang, X. & Hartmaier, A. (2022). Effect of microstructure heterogeneity on the mechanical properties of friction stir welded reduced activation ferritic/martensitic steel. *Scripta Materialia*, *207*, 114306. https://doi.org/10.1016/j.scriptamat.2021.114306.

Mecking, H. & Kocks, U.F. (1981). Kinetics of flow and strain-hardening. *Acta Metallurgica*, *29*(11), 1865–1875. https://doi.org/10.1016/0001-6160(81)90112-7.

Pietrzyk, M. (2000). Finite element simulation of large plastic deformation. *Journal of Materials Processing Technology*, *106*(1–3), 223–229. https://doi.org/10.1016/S0924-0136(00)00618-X.

Piwowarczyk, M., Wolanska, N., Pietrzyk, M., Rauch, Ł., Kuziak, R. & Zalecki, W. (2022). Phase transformation model for adjusting the cooling conditions in Stelmor process to obtain the targeted structure of thermomechanically rolled wire rod used for fastener production. *Metallurgical Research and Technology*, *119*, 517. https://doi.org/10.1051/metal/2022071.

Poloczek, Ł., Kuziak, R., Pidvysots'kyy, V., Szeliga, D., Kusiak, J. & Pietrzyk, M. (2022). Physical and numerical simulations to predict distribution of microstructural features during thermomechanical processing of steels. *Materials*, *15*(5), 1660. https://doi.org/10.3390/ma15051660.

Riljak, S. (2006). *Numerical Simulation of Shape Rolling* [PhD thesis]. Royal Institute of Technology, Stockholm.

Roucoules, C., Pietrzyk, M. & Hodgson, P.D. (2003). Analysis of work hardening and recrystallization during the hot working of steel using a statistically based internal variable method. *Materials Science and Engineering A*, *339*(1–2), 1–9. https://doi.org/10.1016/S0921-5093(02)00120-X.

Sandström, R. & Lagneborg, R. (1975). A model for hot working occurring by recrystallization. *Acta Metallurgica*, *23*, 387–398. https://doi.org/10.1016/0001-6160(75)90132-7.

Sellars, C.M. (1979). Physical metallurgy of hot working. In C.M. Sellars, G.J. Davies (Eds.), *Hot Working and Forming Processes* (pp. 3–15). The Metals Society.

Szeliga, D., Czyżewska, N., Klimczak, K., Kusiak, J., Morkisz, P., Oprocha, P., Pietrzyk, M. & Przybyłowicz, P. (2021). Sensitivity analysis, identification and validation of the dislocation density based model for metallic materials. *Metallurgical Research and Technology*, *118*(3), 317. https://doi.org/10.1051/metal/2021037 .

Szeliga, D., Czyżewska, N., Klimczak, K., Kusiak, J., Kuziak, R., Morkisz, P., Oprocha, P., Pidvysotsk'yy, V., Pietrzyk, M. & Przybyłowicz, P. (2022a). Formulation, identification and validation of a stochastic internal variables model describing the evolution of metallic materials microstructure during hot forming. *International Journal of Material Forming*, *15*, 53. https://doi.org/10.1007/s12289-022-01701-8.

Szeliga, D., Czyżewska, N., Klimczak, K., Kusiak, J., Kuziak, R., Morkisz, P., Oprocha, P., Pietrzyk, M., Poloczek, Ł. & Przybyłowicz, P. (2022b). Stochastic model describing evolution of microstructural parameters during hot rolling of steel plates and strips. *Archives of Civil and Mechanical Engineering*, *22*(3), 139. https://doi.org/10.1007/s43452-022-00460-2.

Wisselink, H.H., Huétink, J., Dijk, M.H.H., van, & Leeuwen, A.J., van (2001). 3D FEM Simulations of a shape rolling process. In A.-M. Hebraken (Ed.), *Proceedings of the 4th International ESAFORM Conference on Material Forming. Liège, Belgium, April 23–25, 2001* (pp. 843–846). University of Liège.

Yanagimoto, J., Ito, T. & Liu, J. (2000). FE-based analysis for the rolling microstructure evolution in hot bar. *ISIJ International, 40*(1), 65–70. https://doi.org/10.2355/isijinternational.40.65.